Since January 2020 Elsevier has created a COVID-19 resource centre with free information in English and Mandarin on the novel coronavirus COVID-19. The COVID-19 resource centre is hosted on Elsevier Connect, the company's public news and information website.

Antiviral Research 90 (2011) 64–69

Contents lists available at ScienceDirect

Antiviral Research

journal homepage: www.elsevier.com/locate/antiviral

Emodin inhibits current through SARS-associated coronavirus 3a protein

Silvia Schwarz [a], Kai Wang [b,c], Wenjing Yu [b,c], Bing Sun [b,c], Wolfgang Schwarz [a,d,e,*]

[a] Shanghai Research Center for Acupuncture & Meridians, 199 Guoshoujing Rd., Shanghai 201203, China
[b] Molecular Virus Unit, Key Laboratory of Molecular Virology and Immunology, Institute Pasteur of Shanghai, Chinese Academy of Sciences, Shanghai Institutes of Biological Sciences, 225 South Chongqing Road, Shanghai, 200025, China
[c] Laboratory of Molecular Cell Biology, Institute of Biochemistry and Cell Biology, Shanghai Institutes of Biological Sciences, Chinese Academy of Sciences, 320 Yueyang Road, Shanghai 200031, China
[d] Max-Planck-Institute for Biophysics, Max-von-Laue-Str. 3, 60438 Frankfurt am Main, Germany
[e] Institute for Biophysics, Goethe-University, Max-von-Laue-Str. 1, 60438 Frankfurt am Main, Germany

ARTICLE INFO

Article history:
Received 21 October 2010
Received in revised form 15 February 2011
Accepted 21 February 2011
Available online 26 February 2011

Keywords:
3a protein
Corona virus
Emodin
Voltage clamp
Ion channel
Virus release

ABSTRACT

The open-reading-frame 3a of SARS coronavirus (SARS-CoV) had been demonstrated previously to form a cation-selective channel that may become expressed in the infected cell and is then involved in virus release. Drugs that inhibit the ion channel formed by the 3a protein can be expected to inhibit virus release, and would be a source for the development of novel therapeutic agents. Here we demonstrate that emodin can inhibit the 3a ion channel of coronavirus SARS-CoV and HCoV-OC43 as well as virus release from HCoV-OC43 with a $K_{1/2}$ value of about 20 μM. We suggest that viral ion channels, in general, may be a good target for the development of antiviral agents.

1. Introduction

Several viral genomes encode for transmembrane proteins that may form channels in the membrane of the infected cell (see e.g. (Fischer and Hsu, 2011)) and that play a crucial role in virus life cycle These membrane proteins are considered as new targets for antiviral drugs (Liang and Li, 2010; Wang and Sun, 2011).

Severe acute respiratory syndrome (SARS) first appeared in 2002 in China. In mainland China about 50% of patients were treated with Chinese herbal medicine as an adjunct therapy in addition to Western medicine (see (Zhang et al., 2004)), and some positive effects in SARS patients had been reported (see (Liu et al., 2008)). By screening a large number of Chinese herbs (Ho et al., 2007) emodin was identified as an effective component of *Polygonaceae* to block the interaction of the SARS-coronavirus spike protein (SARS-CoV S protein) with the angiotensin-converting enzyme 2 (ACE2) and to reduce the infection by S protein-pseudo-typed retrovirus. The ACE2 was shown to be a functional receptor for SARS-CoV (Kuhn et al., 2004; Li et al., 2003) with a specific binding domain of the S protein (Babcock et al., 2004; Wong et al., 2004).

SARS-CoV had been shown to exhibit an open reading frame ORF-3a that codes for an ion-permeable channel in the infected cells; the activity of the 3a protein may influence virus release (Lu et al., 2006). The ion channel is permeable for monovalent cations with higher permeability for K^+ than for Na^+. Ba^{2+} in the external solution effectively can block the channel. The ORF-3a is also named "New gene" localized between "spike and envelope gene" (SNE) (Zeng et al., 2004), and has been identified also in other coronaviruses (Lu et al., unpublished, see also (Wang and Sun, 2011)). This includes the SNE of the human coronavirus OC43 (HCoV-OC43) which shows similar ion-channel characteristics as the 3a protein of SARS-CoV.

Here we show that emodin is an inhibitor of the SNE-encoded 3a protein as an ion channel. This new observation together with the finding that emodin may disrupt the interaction of S protein and ACE2 (Ho et al., 2007) support the suggestion that emodin or derivatives may become potent new therapeutic agents in treatment of SARS and other coronavirus-induced diseases. Since the genomes of various other viruses also encode for ion channels, our findings strengthens the view that viral ion chan-

* Corresponding author. Institute for Biophysics/Goethe-University, Max-von-Laue-Str. 1, Frankfurt am Main 600438, Germany. Tel.: +49 0 171 469 0647; fax: +49 0 3212 888 3496.
E-mail address: schwarz@biophys.eu (W. Schwarz).

0166-3542/$ – see front matter © 2011 Elsevier B.V. All rights reserved.
doi:10.1016/j.antiviral.2011.02.008

nels, in general, are interesting targets for developing antiviral drugs.

2. Methods and materials

2.1. Expression of 3a protein in Xenopus oocytes

We used the expression system *Xenopus* oocyte as a model system (Gurdon et al., 1971) to investigate the effect of emodin on SNE-3a protein. Females of the clawed toad *Xenopus laevis* (Maosheng Bio-Technology Com., Shanghai, China) were anaesthetized with 1 g/l H_2O tricane (MS222, Sandoz, Basel, Switzerland) or in ice water. Parts of the ovary were removed and treated with 0.3 units per ml liberase (Roche) for 3 h to remove enveloping tissue and to obtain isolated oocytes. For expression of HCoV-O43 or SARS-CoV 3a protein the respective cDNA was cloned into pNWP vector (for details see (Lu et al., 2006)), and cRNA was synthesized using mMESSAGE mMACHINE high-yield capped RNA transcription SP6 kit (Ambion, Austin, TX, USA). Expression of the protein in oocytes and infected cells had been demonstrated previously ((Lu et al., 2006), Lu et al., unpublished). Oocytes of stage V or VI (Dumont, 1972) were selected and injected with cRNA (20 ng per oocyte); these cells were stored together with uninjected control oocytes for 2 days at 19 °C in oocyte Ringer's-like solution (ORi, see Section 2.6). Experiments were performed at room temperature (24–26 °C).

2.2. Voltage–clamp experiments

We applied conventional two-electrode voltage clamp using Turbo TEC-03 with CellWorks software (NPI electronic, Tamm, Germany) to measure the current mediated by SNE-3a protein. To determine steady-state current–voltage dependencies (IV curves), membrane currents were averaged during the last 20 ms of 200-ms, rectangular voltage pulses from −150 to +30 mV in 10-mV increments that were applied from a holding potential of −60 mV. The difference of steady-state current in the presence and absence of 20 mM $BaCl_2$ was determined.

2.3. Cell culture and virus infection

To investigate virus release from infected cells, we used Rhabdomyosarcoma cells (RD cells, ATCC accession no. CCL-136, Manassas, VA, USA) that were maintained in Dulbecco's modified Eagle's essential medium (Gibco, NY, USA) supplemented with 10% fetal bovine serum and cultured at 37 °C in a humidified atmosphere with 5% CO_2. For infection we used the coronavirus HCoV-OC43, which also codes in its genome for a 3a-like protein that forms an ion channel (Lu et al., unpublished). Experiments with HCoV-OC43 could be performed in our Biosafety Level 2 Laboratory. HCoV-OC43 (VR-1558) was purchased from American Type Culture Collection (ATCC, Manassas, VA, USA). Virus adsorption was carried out for 1 h in medium without serum. Cells were then washed with PBS and cultured with medium supplemented with 2% fetal bovine serum and various concentrations of emodin for 40 h at 33 °C. Hence the emodin was added after the virus absorption was carried out. Since the emodin stock solution was prepared in dimethylsulfoxide (DMSO), control experiments were conducted in the absence of emodin, but in the presence of the respective concentrations of DMSO indicating that up to 0.5% DMSO had no significant effect on virus release. Only for the highest concentration (1%), which was applied when using 100 μM emodin, an inhibition of virus release by 20% could be detected; in the presence of the 100 μM emodin virus release was completely inhibited (see Section 3.3).

2.4. Measurement of virus

Viral genomic RNA was collected from virus-containing cell supernatants using the QIAamp® viral RNA Mini Kit (QIAGEN, Hilden, Germany). Total RNA from virus-infected cells was extracted using Trizol (Invitrogen, Carlsbad, CA, USA) following manufacturer's instruction. A370-bp fragment was amplified by one-step RT-PCR, which was performed with specific HCoV-OC43 primer pairs that amplify part of the nucleocapsid protein (N) gene. Copies of viral RNA in cell supernatants and in infected cells were determined by real time PCR with Qiagen One Step RT-PCR Kit (QIAGEN, Hilden, Germany) in triplicate as described by the manufacturer. HCV-OC43 was amplified using the primer pairs (Sangong, Shanghai, China):

sense: AGGAAGGTCTGCTCCTAATTC; antisense: TGCAAAGATGGGGAACTGTGGG.

The supernatants were centrifuged for 5 min at 1000 × *g*, and then immediately frozen at −80 °C and stored until assayed to determine infectious virus titers of samples. RD cells in 96-well plates (Costar, Cambridge, MA) were inoculated with serial 10-fold dilutions of sample and incubated for 5 days at 33 °C. The 50% tissue-culture infective dose ($TCID_{50}$) was determined by the method of Reed and Muench (1938).

2.5. Plaque reduction assay

RD cells were cultured in 6-well plates and infected with HCoV-OC43 for 1 h following the procedures reported previously (Schmidt et al., 1979); then virus suspension was removed, cells were washed with PBS (Beyotime, Jiangsu, China), and cell culture medium, containing 0.8% SeaPlaque agarose (Lonza, Rockland, ME, USA) and various concentrations of emodin, was added to the wells. Cells were then incubated at 33 °C for 5 days. After the removal of agarose medium, cell monolayers were fixed in 10% formaldehyde and stained with 0.1% crystal violet.

2.6. Solutions

Standard ORi solution contained: 90 mM NaCl, 2 mM KCl, 2 mM $CaCl_2$ and 5 mM Hepes (pH 7.4). Since the 3a protein channel showed high permeability to K^+ (Lu et al., 2006), the test solution S1 contained: 100 mM KCl, 1 mM $MgCl_2$, and 5 mM Hepes (pH 7.4); Ca^{2+} was omitted (but partially replaced by Mg^{2+}) to reduced background currents from endogenous Ca^{2+}-activated channels. Test solution S2 contained in addition 10 mM $BaCl_2$, and the Ba^{2+}-sensitive current was determined as the difference between the current measured in S1 and S2. Both solutions, S1 and S2, contained some ethanol or DMSO (see below).

Emodin (Zelang Medicine-Technology Com., Nanjing, China, or Sigma, St. Louis, MO, USA) stock solution of 10 mM was prepared in 70% ethanol or DMSO, and diluted to final working concentration in solution S1 and S2, which will be named in the following S1+ and S2+, respectively. The emodin-free test solutions S1 and S2 also contained respective concentrations of ethanol or DMSO. Ethanol and DMSO was in all electrophysiological experiments below 0.5%, a concentration that did not affect membrane currents in *Xenopus* oocytes.

3. Results

3.1. Membrane currents in control oocytes are insensitive to emodin

Ba^{2+}-sensitive current was determined as the difference of membrane current in the absence and presence of Ba^{2+}. To correct

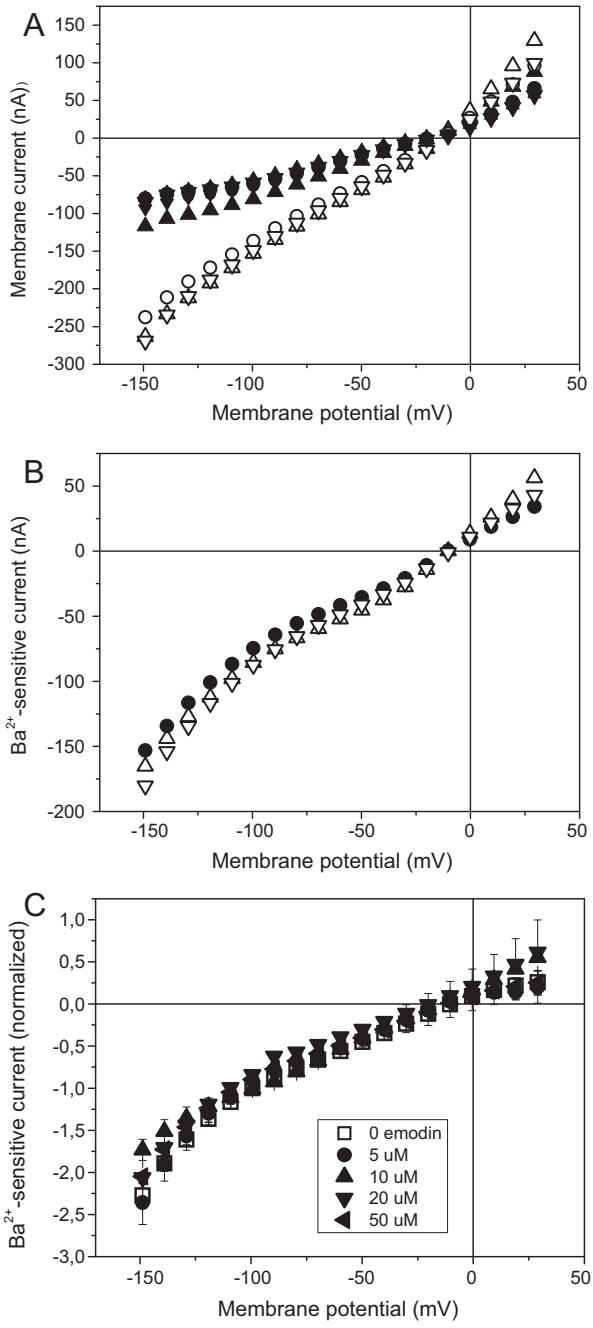

Fig. 1. Typical current–voltage dependencies of steady-state current of a control oocytes. (A) Original current–voltage dependencies. The sequence of solutions was S2(filled triangles up) – S1(open triangles up) – S2(filled triangles up) → S2 + (filled circles) – S1 + (open circles) – S2 + (filled circles) → S2(filled triangles down) – S1(open triangles down) – S2(filled triangles down). The + signs stay for application of 50 μM emodin. (B) Calculated Ba^{2+}-sensitive current (Eq. (1)) before and after application of emodin (open triangles up and down, respectively) and during application (filled circles). (C) Averaged Ba^{2+}-sensitive currents from 4 oocytes in the absence of emodin (open circles, averaged from before and after emodin application) and in the presence of different concentrations of emodin (filled symbols). Data ±SEM are shown.

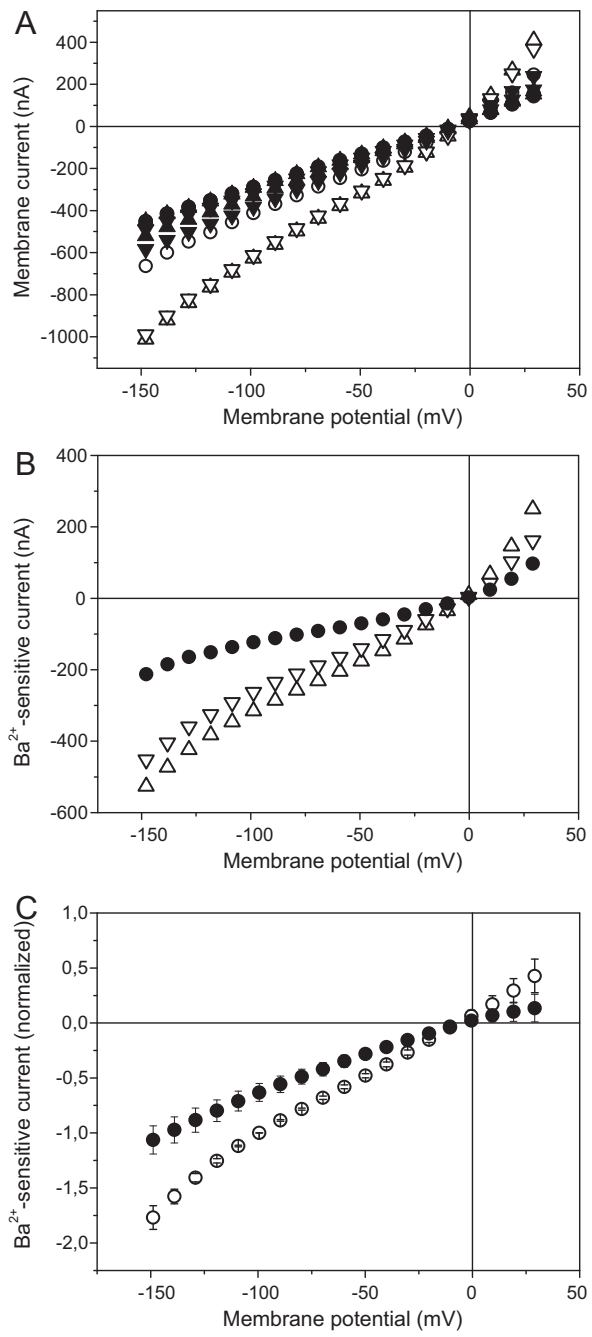

Fig. 2. Typical current–voltage dependencies of steady-state current of a 3a-protein expressing oocytes. (A) Original current–voltage dependencies. The sequence of solutions was S2(filled triangles up) – S1(open triangles up) – S2(filled triangles up) → S2 + (filled circles) – S1 + (open circles) – S2 + (filled circles) → S2(filled triangles down) – S1(open triangles down) – S2(filled triangles down). The + signs stay for application of 50 μM emodin. (B) Calculated Ba^{2+}-sensitive currents before and after application of emodin (open triangles up and down, respectively) and during application (filled circles). (C) Averaged Ba^{2+}-sensitive currents from 10 oocytes in the absence of emodin (open circles, averaged from before and after emodin application) and in the presence of 50 μM emodin (filled circles). Data ±SEM are shown.

for possible drift with time, the current was calculated according to:

$$I_{\text{Ba-sensitive}} = \frac{S1_{\text{before}} - S1_{\text{after}}}{2} - S2 \quad (1a)$$

or

$$I_{\text{Ba-sensitive}} = S1 - \left(\frac{S2_{\text{before}} - S2_{\text{after}}}{2}\right) \quad (1b)$$

Oocytes not expressing 3a protein also exhibited Ba^{2+}-sensitive currents; the example in Fig. 1A shows IV curves for the solution sequence

S2 → S1 → S2 → S2+ → S1+ → S2+ → S2 → S1 → S2.

For the same experiment, the Ba^{2+}-sensitive currents were determined according to Eq. (1) (Fig. 1B), which shows that

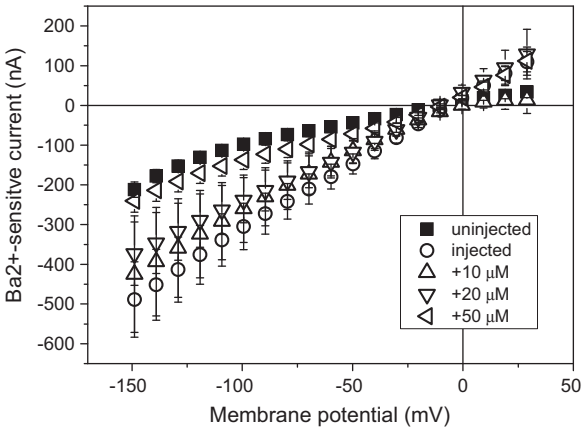

Fig. 3. Current–voltage dependencies of averaged Ba^{2+}-sensitive currents Averaged currents in the absence of emodin (open circles, averaged from before and after emodin application) and in the presence of different concentration of emodin. Data represent averages from 13 uninjected control oocytes and 18 cRNA-injected oocytes ±SEM.

application of 50 μM emodin had no effect on the endogenous Ba^{2+}-sensitive current component. After the emodin application, the solution sequence in the absence of emodin was repeated (see Fig. 1A and B) for further drift corrections. Fig. 1C shows averaged Ba^{2+}-sensitive IV dependencies in the absence of emodin (averaged from before and after emodin application) and in the presence of emodin in the concentration range of 5–50 μM. Clearly, the endogenous Ba^{2+}-sensitive current of *Xenopus* oocytes was insensitive to emodin even at 50 μM.

3.2. Membrane currents in oocytes expressing SARS-CoV 3a protein are sensitive to emodin

Oocytes expressing SARS-CoV 3a protein could easily be identified since they showed much larger currents (Fig. 2A), and a Ba^{2+}-sensitive current became apparent that was at least by a factor of 2 larger than in the control oocytes (compare Fig. 2B with Fig. 1B). This additional current could strongly be inhibited by emodin as illustrated in the example shown in Fig. 2B for 10 μM. Fig. 2C shows the result of averaged current–voltage curves of Ba^{2+}-sensitive current in the absence and presence of 10 μM emodin.

Fig. 3 shows in addition to 10 μM emodin the effect of 20 and 50 μM on averaged IV curves of Ba^{2+}-sensitive current. The large error bars reflect variability in 3a-mediated current and hence mainly the degree of expression of 3a protein, but to a small extend also variability in cell size. For further analysis, endogenous Ba^{2+}-sensitive current determined from uninjected control oocytes of the same batches of cells was, therefore, first subtracted from the total Ba^{2+}-sensitive current measured in 3a-protein expressing cells. Thereafter, the IV curves were normalized to the current at −100 mV in absence of emodin. The effect of emodin on the 3a-mediated current at −100 mV is illustrated in Fig. 4 (open circles). To estimate the sensitivity for emodin of the SARS-CoV 3a-mediated current I_{3a}, the equation

$$I_{3a} = \frac{K_{1/2}}{K_{1/2} + [\text{emodine}]} \quad (2)$$

was fitted to the data. A 50% inhibition was obtain at about $K_{1/2}$ = 18 μM emodin (see open circle and solid line in Fig. 4).

3.3. Virus release is sensitive to emodin

Since infection of mammalian cells with SARS virus requires Biosafety Level 3 Laboratory, we tested the effect of emodin on virus release using HCoV-OC43. HCov-OC43 also has SNE gene that can form an ion channel with similar ion selectivity as the SARS-CoV SNE gene (Lu et al. unpublished). RD cells were first infected with the coronavirus HCoV-OC43 at multiplicity of infection (moi) 1, and thereafter, incubated with different concentrations of emodin (see Section 2). Three days post infection, the typical cytopathic effect (CPE) was observed under a light microscope; the virus-induced CPE was obviously reduce in the presence of 8 μM emodin (Fig. 5A). In addition, the plaque reduction assay showed that emodin decreased the number and size of plaques in a dose-dependent manner; plaques were hardly detectable at 8 μM (Fig. 5B). These results suggest an antiviral effect of emodin on HCoV-OC43 in the RD cell culture system after the infection.

The number of viral RNA copies was determined in the supernatant to estimate to which extent viruses were released from the infected cells. Fig. 4 (open squares) shows the dependence on emondin concentration. Increasing emodin led to reduced RNA indicating emodin-dependent inhibition of virus release. The dependence of virus release on emodin concentration could be fitted together with the 3a-mediated current by Eq. (2) with the same

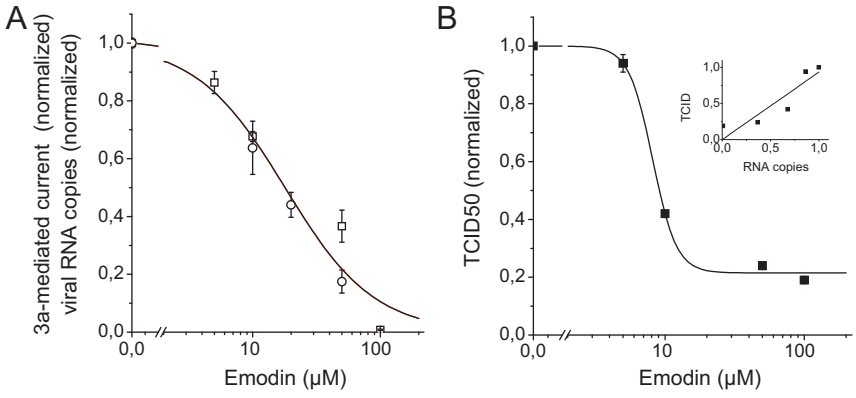

Fig. 4. Effect of emodin on (A) 3a-protein-mediated current at −100 mV, relative numbers of viral RNA copies, and (B) tissue-culture infective dose ($TCID_{50}$). (A) Ba^{2+}-sensitive current of non-injected oocytes was subtracted from total Ba^{2+}-sensitive current of oocytes injected with cRNA of 3a protein (open circles); the normalized data represent averages from 21 oocytes ±SEM. Numbers of viral RNA copies were detected in the supernatant after incubation in different concentrations of emodin (open squares); the normalized data represent averages from 3 sets of experiments ± SEM. The solid line represents a fit of equation 2 to both data sets with $K_{1/2}$ = 17.9 ± 2.6 μM. (B) $TCID_{50}$ values (filled squares) are normalized data averaged from 3 determinations ± SEM. For symbols without visible error bar the error is within the symbol size; the solid line is drawn as an approximation of the concentration dependence. The inset illustrates the correlation between $TCID_{50}$ and extracellular viral RNA copies (r = 0.91).

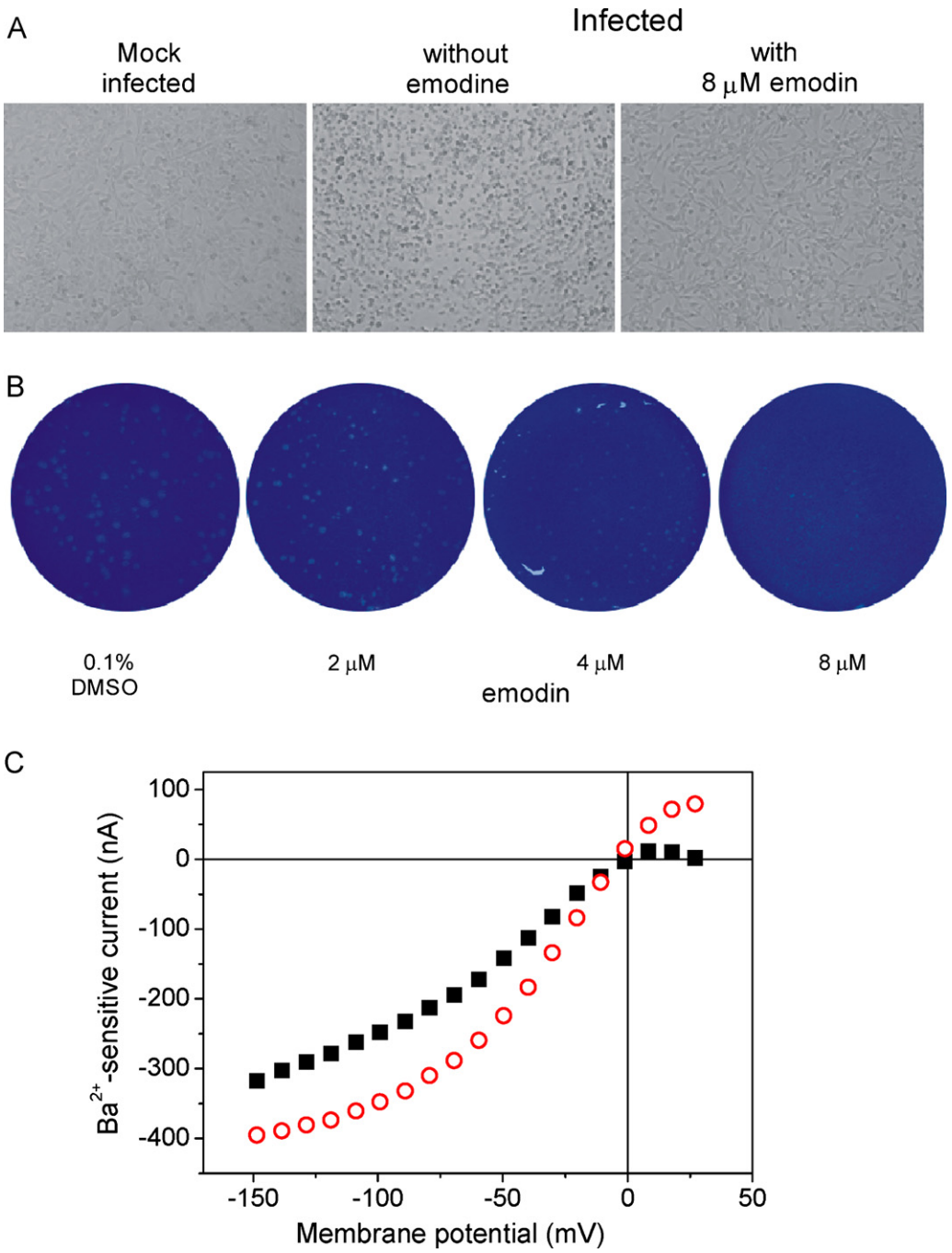

Fig. 5. Effect of emodin on RD cells infected with HCoV-OC43. (A) Mock- and corona-virus-HCoV-OC43-infected RD cells were observed under light microscope three days after infection. Infected cells were incubated in the absence or presence of 8 μM emodin. (B) Plaque reduction assay of RD cells that were infected with HCoV-OC43 at 2, 4 and 8 μM emodin in the incubation medium. (C) Voltage dependence of Ba^{2+}-sensitive current in an OC43-cRNA-injected oocyte in the absence (open circles) and in the presence of 20 μM emodin (filled squares).

$K_{1/2}$ values of about 18 μM. The number of intracellular RNA copies was less sensitive to emodin, and clear inhibition to 48 ± 4 and $6 \pm 3\%$ was detected only at the highest concentrations of 50 and 100 μM emodin.

Titers of infectious virus in the supernatants of infected cultures were determined using the $TCID_{50}$ assay and are expressed in $\log_{10}$ ($TCID_{50}$/ml) (Fig. 4B). The decrease of $TCID_{50}$ by emodin correlates with the decrease of extracellular viral RNA copies with a correlation coefficient of $r = 0.91$ (compare inset of Fig. 4B).

3.4. Membrane currents in OC43-cRNA-injected oocytes are sensitive to emodin

The genome of HCoV-OC43 encodes also for a SNE-3a-like protein, which forms an ion-channel (Lu et al., unpublished); we confirmed in a few orientating experiments that the HCoV-OC43 channel is also sensitive to emodin. Fig. 5C shows as an example the inhibition of current by 20 μM emodin. After subtracting the endogenous Ba^{2+}-sensitive current, data analysis of the remaining OC43-mediated current yielded an inhibition at 20 μM emodin to

$56 \pm 3\%$ ($n = 4$) indicating similar sensitivity to emodin as the 3a protein of SARS virus.

4. Discussion

Emodin had recently been identified as an effective component of *Polygonaceae* to block the interaction of the SARS-CoV S protein with the ACE2 and the infection by S protein-pseudo-typed retrovirus (Ho et al., 2007). The $K_{1/2}$ value for blocking the binding of the S protein to ACE2 was 200 μM. On the other hand, the authors reported that already 50 μM emodin gave 80% inhibition of relative infectivity.

The work of Lu et al. (2006) has shown that the SNE-3a protein of SARS-CoV forms an ion channel, and its activation may be involved in virus release from the infected cell. Hence, inhibition of the 3a channel can be expected to counteract virus release. Here we have demonstrated that emodin is a potent inhibitor of the 3a channel with a $K_{1/2}$ value of about 20 μM. The reduction of extracellular viral RNA copies by emodin reflects inhibition of virus release. At high concentrations of emodin also intracellular levels of viral RNA copies were reduced suggesting that the high concentrations may also inhibit other stages of the virus life cycle. The discrepancy between the reported $K_{1/2}$ value of 200 μM for inhibition of S protein and ACE2 and the 80% inhibition of infectivity at already 50 μM (Ho et al., 2007) might be explained by our observation that the block of 3a protein contributes to spread of virus infection in addition to the effect on S protein/ACE2 interaction.

Ho et al. (2007) suggested that emondin may act as an antiviral drug by blocking virus infection. In our experiments we applied the emodin only after the virus absorption was carried out; in addition, the HCoV-OC43 appears to bind to cells via N-acetyl-neuramic acid (Vlasak et al., 1988), which is different from the S protein/ACE2 interaction (Babcock et al., 2004; Wong et al., 2004). Therefore, we suggest that emodin may contribute to reduced virus release from the SARS-CoV-infected cell through inhibition of the current mediated by 3a protein. Indeed, emodin inhibited HCoV-OC43 release from infected RD cells with similar effectiveness of $K_{1/2} \approx 20$ μM for inhibition of SNE-3a protein of SARS-CoV and HCoV-OC43. Reduced virus release from infected cells may provide to the immune system sufficient time to effectively respond to the infection. Emodin or derivatives hence may open the door to novel therapeutics in treatment of SARS and other coronaviruses with SNE gene.

It has been shown previously that p7 protein of hepatitis C virus and M2 of influenza virus can also form ion channels in cell membranes (Griffin et al., 2004). These channels are sensitive to amantadine, and it was suggested that inhibition of the ion channel activity may affirm the protein as a target for future antiviral therapy. However, amantadine-resistant influenza virus is on the rise though amantadine-resistant mutant residues have been found in locations surrounding the high affinity site in the M2 region (Cady et al., 2010). Amantadine has failed to have clinically significant antiviral effect in patients where blood concentrations of 1–2 μM are the highest that can be achieved (von Wagner et al., 2008). Wozniak et al. (2010) Wozniak et al.'s (2010) work showed that amantadine is ineffective at the concentrations achieved clinically and thus improved agents targeting the p7 channel activity may have therapeutic potential.

In conclusion, we like to support the idea that viral ion channels may be involved in mechanism of viral release from infected cells, and hence form a potential target for therapeutic drugs. Emodin, in particular, may form a basis for drug development against coronavirus infections.

Acknowledgements

The authors thank Dr. Quanbao GU for his advice throughout the course of the experiments, and Huimig DU for his excellent technical assistance.

References

Babcock, G.J., Esshaki, D.J., Thomas Jr., W.D., Ambrosino, D.M., 2004. Amino acids 270 to 510 of the severe acute respiratory syndrome coronavirus spike protein are required for interaction with receptor. J. Virol. 78, 4552–4560.

Cady, S.D., Schmidt-Rohr, K., Wang, J., Soto, C.S., DeGrado, W.F., Hong, M., 2010. Structure of the amantadine binding site of influenza M2 proton channels in lipid bilayers. Nature 463, 689–692.

Dumont, J.N., 1972. Oogenesis in "*Xenopus laevis*" (Daudin): I. stages of oocyte development in laboratory maintained animals. J. Morphol. 136, 153–180.

Fischer, W., Hsu, H.J., 2011. Viral channel forming proteins—modeling the target. Biochim. Biophys. Acta 1808, 561–571.

Griffin, S.D., Harvey, R., Clarke, D.S., Barclay, W.S., Harris, M., Rowlands, D.J., 2004. A conserved basic loop in hepatitis C virus p7 protein is required for amantadine-sensitive ion channel activity in mammalian cells but is dispensible for localization to mitochondria. J. Gen. Virol. 85, 451–461.

Gurdon, J.B., Lane, C.D., Woodland, H.R., Marbaix, G., 1971. Use of frog eggs and oocytes for the study of messenger RNA and its translation in living cells. Nature 233 (September), 177–182.

Ho, T.W., Wu, S.L., Chen, J.C., Li, C.C., Hsiang, C.Y., 2007. Emodin blocks the SARS coronavirus spike protein and angiotensin-converting enzyme 2 interaction. Antivir. Res. 74, 92–101.

Kuhn, J.H., Li, W., Choe, H., Farzan, M., 2004. Antiotensin-converting enzyme 2: a functional receptor for SARS coronavirus. Cell. Mol. Life Sci. 61, 2738–2743.

Li, W., Moore, J.M., Vasilleva, N., Sul, J., Wong, K.S., Berne, M.A., Somasundaran, M., Sullivan, J.L., Luzurlaga, K., Greenough, T., Choe, H., Farzan, M., 2003. Angiotensin-converting enzyme 2 is a functional receptor for the SARS coronavirus. Nature 426, 450–454.

Liang, X., Li, Z.Y., 2010. Ion channels as antivirus targets. Virologica Sinica 25, 267–280.

Liu, X.M., Zhang, M.M., He, L., Li, Y.P., Kang, Y.K., 2008. Chinese herbs combined with Western medicine for severe acute respiratory syndrome (SARS). Cochrane Collab. 4.

Lu, W., Zheng, B.J., Xu, K., Schwarz, W., Du, L.Y., Wong, C.K.L., Chen, J.D., Duan, S.M., Deubel, V., Sun, B., 2006. Severe acute respiratory syndrome-associated coronavirus 3a protein forms an ion channel and modulates virus release. Proc. Natl. Acad. Sci. 103, 12540–12545.

Reed, L.J., Muench, H., 1938. A simple method of estimating fifty percent endpoints. AM. J. Epidemol. 27, 493–497.

Schmidt, O.W., Cooney, M.K., Kenny, G.E., 1979. Plaque assay and improved yield of human coronaviruses in a human rhabdomycosarcoma cell line. J. Clin. Microbiol. 9, 722–728.

Vlasak, W., Luytjes, W., Spaan, W., Palese, P., 1988. Human and bovine coronaviruss recognize sialic acid-containing receptors similar to those of influenza C viruses. Proc. Natl. Acad. Sci. 85, 4526–4529.

von Wagner, M., Hofmann, W.P., Teuber, G., Berg, T., Goeser, T., Spengler, U., Hinrichsen, H., Weidenbach, H., Gerken, G., Manns, M., Buggisch, P., Herrmann, E., Zeuzem, S., 2008. Placebo-controlled trial of 400 mg amantadine combined with peginterferon alfa-2a and ribavirin for 48 weeks in chronic hepatitis C virus-1 infection. Hepatology 48, 1404–1411.

Wang, K., Sun, B., 2011. Viral proteins function as ion channels. Biochim. Biophys. Acta 1808, 510–515.

Wong, S.K., Li, W., Moore, M.J., Choe, H., Farzan, M., 2004. A193-amino-acid fragment of the SARS corona virus S protein efficiently binds angiotensin-converting enzyme 2. J. Biol. Chem. 279, 3197–3201.

Wozniak, A.L., Griffin, S., Rowlands, D., Harris, M., Yi, M.K., Lemon, S.M., 2010. Intracellular proton conductance of the hepatitis C virus p7 protein and its contribution to infectious virus production. PLoS Pathog. 6, e1001087, doi:10.1371/journal.ppat.1001087.

Zeng, R., Yang, R.F., Shi, M.D., Jiang, M.R., Xie, Y.H., Ruan, H.Q., Jiang, X.S., Shi, L., Zhou, H., Zhang, L., Wu, X.D., Lin, Y., Ji, Y.Y., Dai, E.H., Wang, X.Y., Si, B.Y., Wang, J., Wang, H.X., 2004. Characterisation of the 3a protein of SARS-associated coronavirus in infected vero E6 cells and SARS patients. J. Mol. Biol. 341, 271–279.

Zhang, M.M., Liu, X.M., He, L., 2004. Effect of integrated traditional Chinese and Western medicine on SARS: a review of clinical evidence. World J. Gastroenterol. 10, 3500–3505.